Materials Physics and Mechanics 47 (2021) 493-500 Received: February 20, 2021

STRUCTURAL AND MAGNETIC PROPERTIES OF ZINC DOPED NICKEL FERRITE $Ni_{(1-X)}Zn_XFe_2O_4$ SYNTHESIZED USING SOL-GEL AUTO-COMBUSTION AND HYDROTHERMAL METHODS

Abhishek Nigam, Deepak Singh, Ankur Sinha, Deepak Sachan, Anisha, Ankur Vishal, Deepak Kumar, Naveen Kumar*

Applied Mechanics Department, Motilal Nehru National Institute of Technology Allahabad, Prayagraj-211004, India

*e-mail: chaudhary56naveen@gmail.com

Abstract. Zinc doped Nickel ferrites with chemical formula $Ni_{(1-x)}Zn_xFe_2O_4$ (x = 0.2, 0.4, 0.6, and 0.8) were synthesized using both Sol-gel auto-combustion and Hydrothermal methods. The synthesized powders were characterized for their physical and magnetic properties. The crystal structure and lattice parameter of these compounds were investigated by X-ray diffraction (XRD) and morphology has been confirmed by Scanning Electron Microscopy (SEM). The magnetic properties of after-calcined nanoparticles were measured at room temperature using a vibrating sample magnetometer (VSM). X-ray diffraction of these samples shows the presence of a single-phase cubic spinel ferrite structure. The VSM analysis indicates that the Zn content has a significant influence on the magnetic properties such as Saturation Magnetization (Ms), Coercivity (Hc), and Remanence (Mr). The doping concentration of Zn increase with an increase of x which causes a significant increase in the Ms from x=0.2 to 0.4 then decrease from x=0.6 to 0.8. A critical Rietveld analysis of XRD reveals the presence of a very small amount of NiO phase along with the ferrite phase. The Rietveld analysis also confirms the crystallite size and lattice parameter.

Keywords: nickel, zinc, spinel ferrite, hydro-thermal, sol-gel

1. Introduction

Ferrites have attracted researchers to be used in many scientific and technological applications. The oxides, especially ferrites have significant consideration from the fundamental scientific interest and also from a practical point of view for growing applications in the magnetic, microwave devices and electronic industry [1]. Sol-gel method is one of the most important methods of preparing inorganic compounds [2]. It is a wet chemical method and involves both physical and chemical processes such as hydrolysis, polymerization, gelation, drying, dehydration, and densification. Many reports indicated that the surface structure and electric/magnetic properties of nano-materials and composites are strongly correlated [3-7]. Ferrites are extensively used in magnetic recording, information storage, imaging, bio-processing, magnetic refrigeration, and magneto-optical devices [8,9]. Ni–Zn ferrite is a magnetic material and is extensively used by the modern electronic industry due to its high electrical resistivity, high values of magnetic permeability, low dielectric loss with high mechanical strength, good chemical stability, and low coercivities. Ferrites also have attractive and significant properties in the area of atomic engineering materials with practical magnetic properties. The efforts are being made to study the various ferrites to

http://dx.doi.org/10.18149/MPM.4732021_10

evaluate the impact of the substitution of the divalent metal ions to modify the properties of these oxides [10]. The coercivity and magnetic properties of Ni doped zinc ferrite along with its structural property have been studied. Spinel ferrite nanoparticles have substantial importance for scientists to examine their structural, electrical, magnetic, and dielectric properties to make the application in information storage systems, magnetic cores, magnetic fluids, sensors, magnetic drug delivery, magnetic, microwave devices, and hyperthermia [11,12]. In order to obtain good microwave absorption properties, element doping is an effective approach [13]. It has also the ability to improve the electromagnetic compatibility performance and reduce electromagnetic emissions [14]. Nickel ferrites are a kind of soft ferromagnetic materials that have high dielectric constant, low power losses, high resistivity, high saturation magnetization, and high initial permeability. It is well known that nickel ferrite has an inverse spinel structure with Ni^{2+} ions at octahedral [B] sites and Fe^{3+} ions equally distributed at tetrahedral [A] and octahedral [B] sites. Whereas, zinc ferrite has a normal spinel structure with Zn^{2+} ions at A-sites and Fe^{3+} ions at B-sites [15]. There are promising techniques for preparing nano ferrites in bulk scale due to the production of homogeneous particles such as sol-gel method, hydrothermal method, co-precipitation method, citrate precursor, ball milling, solid-state reaction, and auto-combustion [16]. Due to the high compositional control and economics involved, in the present work, the sol-gel auto-combustion method is used to get Ni-Zn ferrite nano-particles.

2. Experimentation

Synthesis of zinc doped nickel ferrite by Sol-gel route. The Zinc doped nickel ferrites $Ni_{(1-x)}Zn_xFe_2O_4$ were prepared by the sol-gel auto combustion method using precursors Nickel nitrate hexahydrate $Ni(NO_3)_2.6H_2O$ and Iron nitrate nano hydrate $Fe(NO_3)_2.9H_2O$ and Zinc acetate dihydrate $(CH_3COOZn)_2.2H_2O$ as starting materials. The flow chart of the sol-gel method is shown in Fig. 1. For the synthesis of Ni-Zn spinel ferrite, stoichiometric quantities of metal nitrates were dissolved in deionized water. A controlled pH of 7 is maintained by using 1:1 liquid ammonia (NH_3) solution. The mixed solution was constantly stirred at 80ºC using a magnetic stirrer. This transformed it into a dry gel. The dried gel was auto-combusted until dark-brown powders were obtained. The product was calcined at 750ºC and kept at this temperature for 4 h. The auto-combusted product was crushed in a mortar pestle. The obtained product was characterized by XRD, SEM, VSM. The phase formation of ferrite was investigated by X-ray diffraction (XRD), nanoparticles morphology was checked by Scanning electron microscopy (SEM), Magnetic characterization was examined by a vibrating sample magnetometer (VSM).

Stoichiometric Equation for synthesis of $Ni_{(1-x)}Zn_xFe_2O_4$ (x = 0.2, 0.4, 0.6 and 0.8) by sol-gel route. For x= 0.6 stoichiometric equation is as follows and the procedure of Zn doped Ni ferrite flow diagram is as shown in equation 1.

. (1)

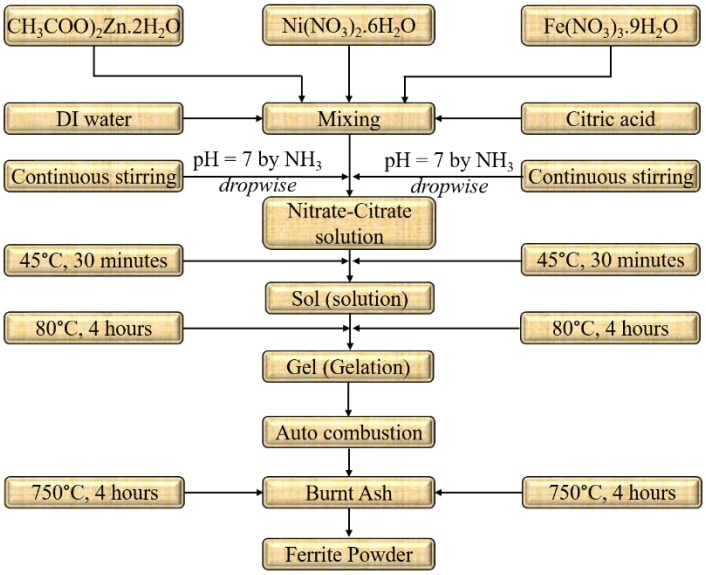

Fig. 1. Flowchart for the synthesis of Ni-Zn spinel ferrites via sol-gel route

Hydrothermal route for the synthesis of Zn doped Ni ferrite. Stoichiometric calculations were done again for the Hydrothermal route for the synthesis of $Ni_{(1-X)}Zn_XFe_2O_4$. Copper nitrate ($Ni(NO_3)_2.3H_2O$), Zinc acetate ($(CH_3COO)_2Zn.2H_2O$), and Iron nitrate ($Fe(NO_3)_3.9H_2O$) were used as precursors. The flow chart of the sol-gel method is shown in Fig. 2. All nitrates were dissolved in a sufficient amount of distilled water to form a clear solution to obtain metal ions solution in separate beakers. NaOH is mixed in the solution to maintain the pH 12.5 with continuous stirring. The temperature of the hotplate was kept at room temperature. Then the solution was stirred for about 2 hours for complete mixing of the metal ions. The solution was poured into a teflon tube and kept at 200ºC for 8 hours in the oven. The precipitate was formed after 8 hours of heating in the oven, this precipitate was filtered with filter paper by using distilled water. The precipitate was again kept in the oven for 24 hours at 60ºC for drying. The pure fine spinel ferrite is formed by grounding the powder using an agate mortar pistol.

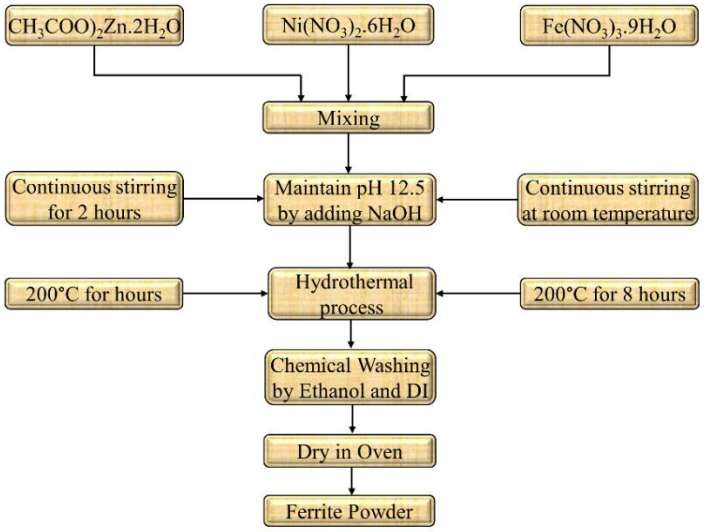

Fig. 2. Flowchart for synthesis of Ni-Zn spinel ferrites via hydrothermal route

3. Results and Discussion

Characterization. Phase identification and structural characterization were performed by X-ray diffraction technique (Target: Cu Kα, 2 theta angle: 10º to 90º, step size: 0.02º, holding time: 0.2 seconds). The XRD pattern shows the well-defined single-phase Zn doped Nickle ferrite structure. The SEM shows the morphology and VSM were done to determine magnetic properties like saturation magnetization, remanence, and coercivity.

Comparison of XRD Results of $Ni_{(1-X)}Zn_XFe_2O_4$ with x = 0.2, 0.4, 0.6 and 0.8. The comparison of XRD results of $Ni_{(1-X)}Zn_XFe_2O_4$ with x= 0.2, 0.4, 0.6, and 0.8 are shown in Fig. 3(a) for sol-gel and Figure 3(b) for hydrothermal. The peaks are highly intense and clearly show the single-phase Zn doped Ni ferrite nanoparticles structure.

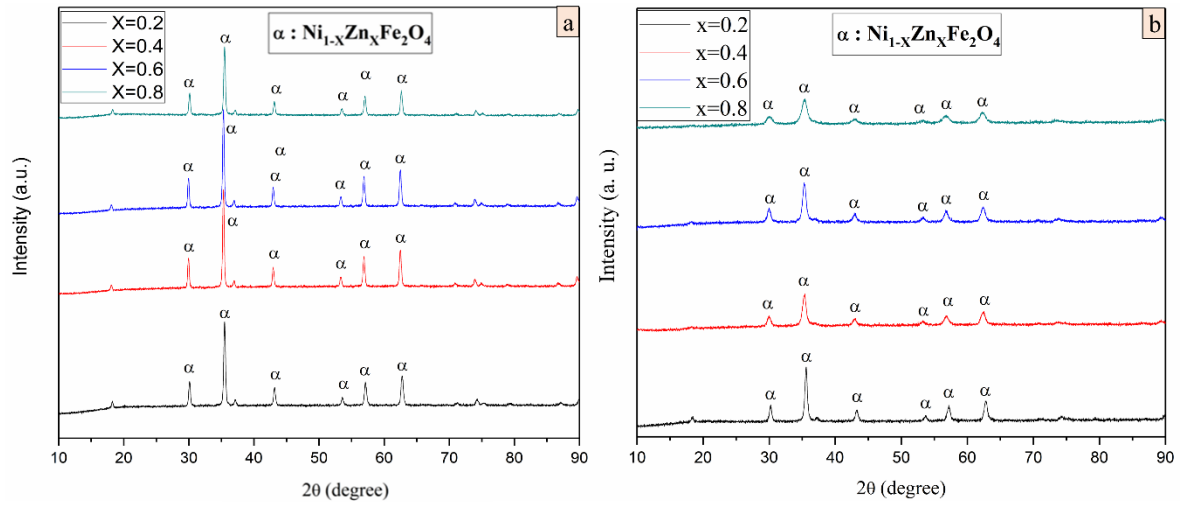

Fig. 3. Comparision of XRD patterns of (a) XRD results for $Ni_{(1-x)}Zn_xFe_2O_4$ (x = 0.2, 0.4, 0.6 and 0.8) through Solgel, and (b)XRD results for $Ni_{(1-x)}Zn_xFe_2O4$ (x = 0.2, 0.4, 0.6 and 0.8) through Hydrothermal

Reitveld Analysis. The Reitveld analysis of Zn doped Ni ferrite by sol-gel method is shown in Fig. 4(a) and by hydrothermal route, it is shown in Fig. 4(b).

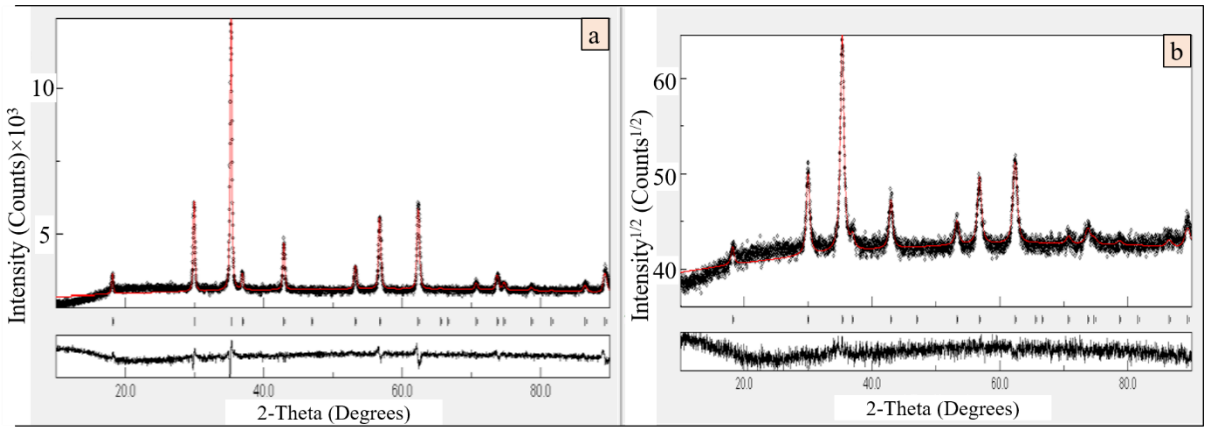

Fig. 4. Maud analysis $Ni_{(1-x)}Zn_xFe_2O_4$ of ferrite for x=0.6 (a) Sol-gel (b) Hydrothermal

XRD Analysis. The XRD result shows that Nickel spinel ferrite prepared by this method is "Single Phase Cubic spinel ferrite" with crystallite size and lattice parameter are

661.45 Å and 8.381 respectively for x=0.2. Similarly, for different compositions (x=0.2, 0.4, 0.6, 0.8), the crystallite size and lattice parameter are calculated and the complete result is listed in the following Table 1 for sol-gel and in Table 2 for the hydrothermal route.

Table 1. Crystallite size and lattice parameter at 750°C by Sol-gel route. hydrothermal route

Sample X	Crystallite size (Å)	Lattice parameter (Å)
0.2	661.45	8.381
0.4	763.84	8.424
0.6	625.99	8.423
0.8	787.08	8.379

Table 2. Crystallite size and lattice parameter at 750°C by hydrothermal route

Sample X	Crystallite size (Å)	Lattice parameter (Å)
0.2	465.06	8.354
0.4	281.01	8.394
0.6	307.30	8.334
0.8	398.99	8.378

SEM. The Scanning Electron Microscopy (SEM) of the Zinc doped Nickle ferrite nanopowder is shown in Fig. 5. The image gives the idea that the product of the auto combustion reaction was highly porous and fluffy, also it confirms that the sub-micrometer-sized primary particles are agglomerated into the larger secondary particles.

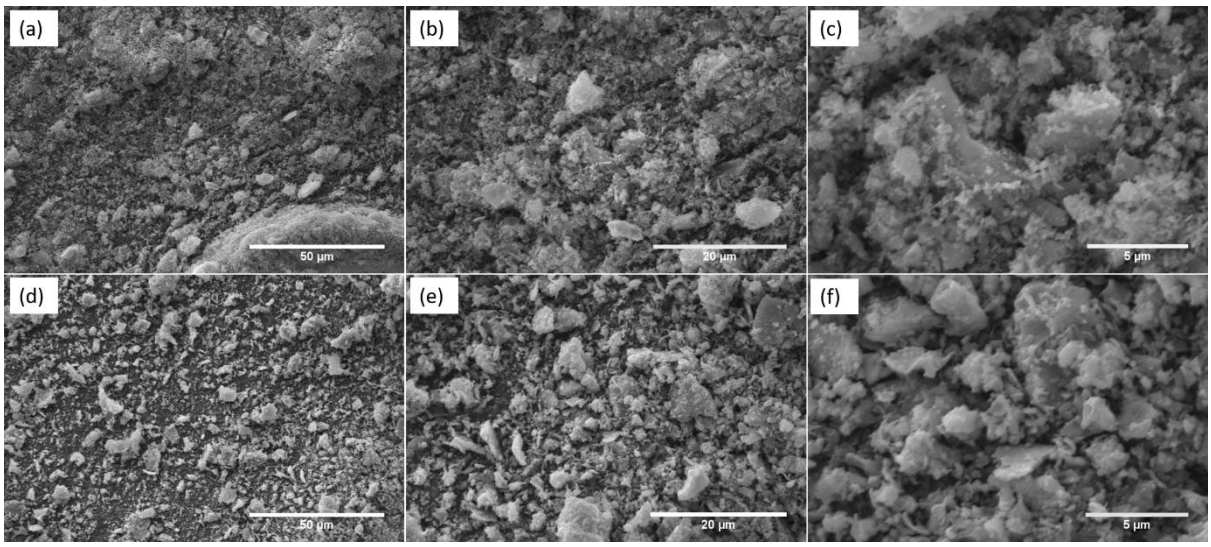

Fig. 5. SEM images of $Ni_{(1-X)}Zn_XFe_2O_4$ (for X=0.2) (a-c) Hydrothermal and (d-f) Sol-gel

Magnetic property. Figure 6 shows the hysteresis plot of all the samples and Table 3 enlists the effect of Zn doping on saturation magnetization (Ms), coercivity (Hc), and remanence (Mr). In the case of Ni Ferrite, the magnetic behavior can be explained by Neel's two sublattice models. According to this model, a spinel having an AB_2O_4 structure, has two types of sublattices, i.e. octahedral (B) and tetrahedral(A) sites. Owing to exchange energy, the ions occupying A and B sites have their magnetic moments arranged in an antiparallel fashion. Here, the Fe^{3+} ions are equally distributed amongst the A and B sites while the Ni^{2+}

ions have a strong preference for B sites. The net magnetic moment is determined by Ni^{2+} (μB=2) ions as the same due to Fe^{3+} (μB=5) ions present at A and B sites cancel out.

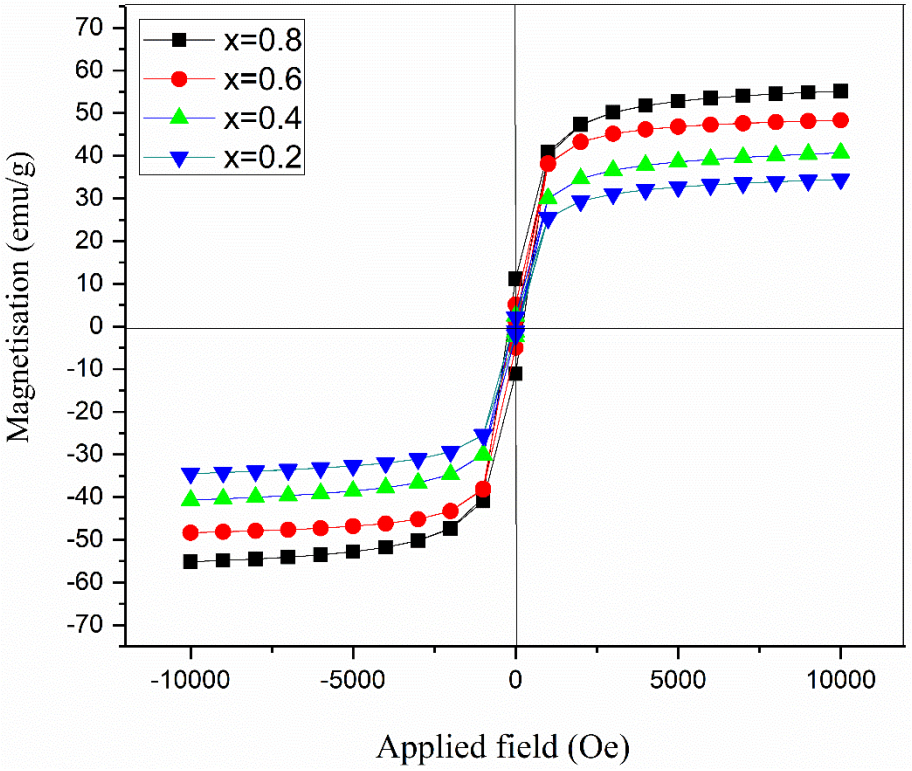

Fig. 6. VSM analysis of $Ni_{(1-x)}Zn_xFe_2O4$ ferrite for (x=0.2, 0.4, 0.6, 0.8)

Table 3. Values of Saturation magnetization (MS), Coercivity (H_C) and Remanence Magnetization (Mr)

Zn doping	M_s (emu/g)	H_c (Oe)	M_r (emu/g)
X=0.2	54.8	216	11.094
X=0.4	48.4	118	5.127
X=0.6	40.07	77.7	2.497
X=0.8	34.5	77.23	2.12

Thus, overall magnetization of the material is the difference in magnetization present at these two sites. Site B dominates as it contains more ions. However, on substituting Ni^{2+} with nonmagnetic Zn^{2+} ions, it is observed that Ms first increases (up to x=0.4) and then decreases (up to x=0.8). This phenomenon can be understood on the basis of the exchange interactions such as A-B, A-A, and B-B, which depend upon the distribution of magnetic and non-magnetic ions in the spinelic network at A and B-sites. In addition to Zn^{2+}, Zn^{2+} having a strong preference for A sites, they are disposedthere. This results in the dislocation of some of Fe^{3+} ions from A to B sites. Unlike in the case of Ni ferrite, the compensation in the magnetic moment of Fe^{3+} will not occur and they contribute with large magnetic moments to B sites. This results in an increase in magnetization. After x=0.4 concentration, the A-B exchange interaction is weakened due to altering in the parallel orientation of the magnetic moments at the B sites, which compensates each other only partially. This results in a progressive decrease in magnetization. Mr and Hc present a decreasing nature with Zn doping. As seen, the minimum value of coercivity is obtained for x=0.8, with a general decreasing trend for

increasing x value. It is possibly due to the alternation of particle and grain size of Ni ferrite before and after Zn doping. Zn doped Ni ferrite, having larger particle size may have more magnetic domain and domain walls, resulting in demagnetization with ease. Also, the anisotropic constant value of Ni ferrite is more than that of Zn ferrite.

4. Conclusions

In this study, Ni doped ferrite nanoparticles have been synthesized through two different routes i.e. Sol-gel and Hydrothermal. The single phase structure of these ferrites was confirmed from XRD. The $Ni_{(1-X)}Zn_XFe_2O_4$ nanoparticles have a Cubic Spinel structure. The lattice constant was observed to increase from 8.3545 Å to 8.4334 Å for values of x in between 0.2 and 0.6. On further increase in Zinc concentration, i.e. for x=0.8, the lattice parameter decreased to 8.3789 Å due to lattice distortion. Magnetic saturation increases for x=0.2 to 0.4 i.e. 34.5 to 54.8 emu/g and then decreases for x=0.6 to 0.8 i.e. 48.4 to 40.7emu/g, with further addition of Zinc concentration as initially it occupies A site and after 0.4 due to saturation of Zn at A sites it occupies B sites. VSM result also shows that Mr and Hc both decreases with an increase in Zinc concentration. The SEM result shows that the highly porous and fluffy nature of Zinc doped Nickle ferrite nanopowder and it also confirms the sub-micrometer-sized primary particles are agglomerated into the larger secondary particles.

Acknowledgements. *Authors are very thankful to Materials Development Laboratory, Applied Mechanics Department, MNNIT Allahabad for providing materials development facilities. Authors are also thankful to CIR Lab, MNNIT Allahabad and IIT BHU for providing characterization facilities.*

References

[1] Hu J, Ma Y, Kan X, Liu C, Zhang X, Rao R, Wang M, Zheng G. Investigations of Co substitution on the structural and magnetic properties of Ni-Zn spinel ferrite. *Journal of Magnetism and Magnetic Materials.* 2020;513: 167200.

[2] Aggarwal N, Narang SB. Magnetic characterization of Nickel-Zinc spinel ferrites along with their microwave characterization in Ku band. *Journal of Magnetism and Magnetic Materials.* 2020;513: 167052.

[3] Gao JM, Cheng F. Study on the preparation of spinel ferrites with enhanced magnetic properties using limonite laterite ore as raw materials. *Journal of Magnetism and Magnetic Materials.* 2018;460: 213-222.

[4] Kumar N, Bharti A, Dixit M, Nigam A. Effect of Powder Metallurgy Process and its Parameters on the Mechanical and Electrical Properties of Copper-Based Materials: Literature Review. *Powder Metallurgy and Metal Ceramics*. 2020;59:401-410

[5] Kumar N, Bharti A, Tripathi H. Investigation of Microstructural and Mechanical Properties of Magnesium Matrix Hybrid Composite. In: *Advances in Mechanical Engineering*. Singapore: Springer; 2020:661-669.

[6] Kumar D, Bharti A, Azam SM, Kumar N, Tripathi H. Investigations of Mechanical Properties of Copper Matrix Hybrid Composite. In: *Advances in Mechanical Engineering*. Singapore: Springer; 2020:671-676.

[7] Kumar N, Bharti A, Gupta MK. Effect of Treatments on Thermo-Mechanical Properties of Epoxy based Sisal Biocomposites. *International Journal on Emerging Technologies*. 2020;11(3): 491-495.

[8] Kumar N, Bharti A, Kumar A, Nigam A. Effect of process parameters on the crystal-parameters of Cu-Zn spinel-ferrites. *Materials physics and mechanics.* 2021;47(1): 65-73.

[9] Kumar N, Singh D, Nigam A, Rajpoot O, Yadav MK, Singh YP, Prakash PS, Singh S. Structural and Magnetic Properties of Zinc Doped Copper Ferrite Synthesized by Sol-Gel and Hydrothermal Route. *Materials physics and mechanics.* 2021;47(2):306-314.
[10] Yadav RS, Kuritka I, Havlica J, Hnatko M, Alexander C, Masilko J, Kalina L, Hajduchova H, Rusnak J, Enev V. Structural, Magnetic, Elastic, Dielectric and Electrical Properties of Hot-Press Sintered Co1-xZnxFe2O4 (x=0.0, 0.5) Spinel Ferrite Nanoparticles. *Journal of Magnetism and Magnetic Materials.* 2017;447: 48-57.
[11] Parashar J, Saxena VK, Jyoti, Bhatnagar D, B.Sharma K. Dielectric behaviour of Zn substituted Cu nano-ferrites. *Journal of Magnetismand Magnetic Materials.* 2015;394: 105-110.
[12] Khudyakov A, Mazur A, Pleshakov I, Bibik E, Fofanov Y, Kuzmin Y, Shlyagin M. Transverse Relaxation of a Nuclear Spin System in Bulk and Nanostructured Magnetically Ordered Materials. In: Proceedings of the 2020 IEEE International Conference on Electrical Engineering and Photonics. EExPolytech; 2020. p.201-203.
[13] Yadav RS, Havlica J, Hnatko M, Sajgalík P, Alexander C, Palou M, Bartonickova E, Bohac M, Frajkorova F, Masilko J, Zmrzly M, Kalina L, Hajduchova M, Enev V. Magnetic properties of Co1-xZnxFe2O4 spinel ferrite nanoparticles synthesized by starch-assisted sol–gel autocombustion method and its ball milling. *Journal of Magnetism and Magnetic Materials.* 2015;378: 190-199.
[14] Kavas H, Baykal A, Demir A, Toprak MS, Aktas B. ZnxCu(12x)Fe2O4 Nanoferrites by Sol–Gel Auto Combustion Route: Cation Distribution and Microwave Absorption Properties. *J Inorg Organomet Polym.* 2014;24: 963-970.
[15] Wu W, Cai J, Wu X, Wang K, Hu Y, Wang Q. Nanocrystalline Cu0.5Zn0.5Fe2O4: Preparation and Kinetics of Thermal Decomposition of Precursor. *J Supercond Nov Magn.* 2013;26: 3523-3528.
[16] Rana MU, Abbas T. The effect of Zn substitution on microstructure and magnetic properties of Cu1-xZnxFe2O4 ferrite. *Journal of Magnetism and Magnetic Materials.* 2002;246(1-2): 110-114.